

Voltage gating of porins from *Haemophilus influenzae* type b

David Dahan ^a, Vincent Vachon ^b, Raynald Laprade ^b, James W. Coulton ^{a,*}

^a Department of Microbiology and Immunology, McGill University, Montréal, Québec, Canada H3A 2B4

^b Groupe de Recherche en Transport Membranaire, Université de Montréal, Montréal, Québec, Canada H3C 3J7

(Received 6 April 1993)

(Revised manuscript received 2 August 1993)

Abstract

The major outer membrane protein of *Haemophilus influenzae* type b (Hib) is porin (M_r 37,782; 341 amino acids). Porins were purified from Hib strains representative of the three outer membrane protein subtypes 1H, 2L and 6U, reconstituted into artificial planar bilayers, and tested for their voltage dependency. At membrane potentials of 50–80 mV, individual Hib 2L and 6U porin channels showed a high probability of undergoing a reversible change to one of several lower conducting substates. Such behaviour was not observed for Hib 1H porin with transmembrane potentials up to 80 mV. The voltage dependence of Hib 2L and 6U porins was asymmetric: it occurred at only one polarity. The asymmetry was also observed for membranes with numerous porins incorporated, suggesting that Hib porin inserted asymmetrically into the bilayer. At macroscopic levels the voltage gating reduced the conductance by 25–50%, implying that the channels closed only partially. Hib 2L porin differs from Hib 1H porin by the substitution Arg¹⁶⁶Gln and Hib 6U porin differs from Hib 1H porin by substitutions at ten amino acids including the change Arg¹⁶⁶Leu. We conclude that substitutions at Arg¹⁶⁶ residue, which is localized to surface-exposed loop number four, are associated with a lowered threshold potential for the voltage gating of Hib porin. This surface-exposed loop may play some role in the conformational changes that occur during voltage gating.

Key words: Porin; Voltage gating; Planar bilayer; Membrane insertion; (*H. influenzae*)

1. Introduction

The outer membrane of Gram-negative bacteria shelters the cell from damaging agents such as antibiotics, bile salts, lysozyme, lipases and proteases. The outer membrane is an asymmetric bilayer: the outer monolayer contains lipopolysaccharides (LPS) as the major lipidic molecule and the inner leaflet contains phospholipids. By means of Ca²⁺-salt bridges, LPS molecules interact with other LPS molecules as well as with outer membrane proteins (OMPs) to form a barrier against hydrophobic compounds [1]. To allow the passage of wastes and nutrients, the outer membrane contains a class of proteins known as porins which

form water-filled transmembrane channels and which allow the diffusion of small hydrophilic compounds.

Porin channels have been identified and characterized in a large number of Gram-negative bacteria [2], as well as in the mitochondria and chloroplasts of eukaryotic cells [3]. Prokaryotic porins and eukaryotic porins have a secondary structure that is almost entirely β -sheet, implying that these evolutionarily distant porins share the antiparallel β -barrel as a channel-forming motif. Molecular weight exclusion, ionic selectivity, voltage dependency and other functional characteristics of porins have been studied by a variety of biochemical, electrophysiological and genetic techniques [3–5]. Reconstitution of *E. coli* porin and *N. gonorrhoeae* porin into artificial membranes revealed that these porins form large channels having weak ionic selectivity. Reconstituted channels do not act as static filters. Rather, in response to stimuli such as an increased membrane potential, they show conformational changes that result in a lowered channel conductance. Although channel conductance is dependent on

* Corresponding author. Fax: +1 (514) 3987052.

Abbreviations: CTB, cetyl trimethylammonium bromide; Hib, *Haemophilus influenzae* type b; FPLC, fast protein liquid chromatography; LOS, lipooligosaccharide; LPS, lipopolysaccharide; OMPs, outer membrane proteins; MAbs, monoclonal antibodies.

channel length and radius [3], the voltage-driven conformational changes that result in a reduced channel conductance are thought primarily to affect channel radius. Complementing the functional information on porin is the recent determination to high resolution of the crystal structures of porins from *E. coli* [6] and *R. capsulatus* [7]. Combining the structural information with the functional information on *E. coli* porin has revealed the molecular basis of pore properties such as molecular weight exclusion and ionic selectivity. However, determination of the crystal structures has not allowed the prediction of the channel dynamics involved in voltage gating [6]. Such a prediction would be facilitated by the identification of residues which, when mutated, result in an altered threshold potential for voltage gating.

We previously showed that porin of *Haemophilus influenzae* type b (Hib) strain ATCC9795 (OMP subtype 1H) has a molecular size exclusion limit for oligosaccharides of 1400 Da [8] and that it forms channels that remain open at membrane potentials of 0–100 mV [9]. To explore the topology of Hib porin, we generated monoclonal antibodies (MAbs) against Hib porin [10] and using synthetic overlapping hexapeptides, we defined the primary epitopes to which the MAbs bound as stretches of 6–11 amino acids [11]. The folding pattern of Hib porin was predicted by calculating the hydrophobicity, amphiphilicity and turn-propensity of the primary sequence. Characterization of the MAbs' ability to recognize porin on whole cells was determined by flow cytometry and provided supportive evidence for the orientation of some loops in the structural model.

To extend our analysis of the biophysics of Hib porin and to determine some structural basis for voltage gating, porins from Hib strains representative of the three major OMP subtypes 1H, 2L and 6U were purified by fast protein liquid chromatography (FPLC) and reconstituted into black lipid membranes. The three species of Hib porins were analyzed for their conductance properties and compared for their voltage dependencies. We show here that the alteration Arg¹⁶⁶Gln, which entails the loss of a surface-exposed positive charge, resulted in an altered threshold potential for the voltage gating of Hib porin.

2. Materials and methods

2.1. Bacterial strains and growth conditions

Three strains of *Haemophilus influenzae* type b were used in this study and they differ according to their OMP subtype: Hib ATCC9795 is OMP subtype 1H [8,10]; Hib strain MCH5539, a clinical isolate provided by Dr. K. Knowles, Montreal Children's Hospital, is

OMP subtype 2L [11]; and Hib strain 1481 is OMP subtype 6U [11,12]. All strains were grown at 37°C on chocolate plates or in liquid media, brain heart infusion plus haemin (1.0 µg/ml) and NAD⁺ (1.0 µg/ml).

2.2. Isolation of Hib porin

Porins were purified from three strains of Hib that are representative of each of the three major OMP subtypes: 1H, 2L and 6U. Porins were extracted with cetyl trimethylammonium bromide (CTB) [8] from each of the three strains and purified by FPLC, as described by Srikumar et al. [10]. The purified porin preparations were quantitated using the bicinchoninic acid assay [13] and subjected to SDS-PAGE [14]. Silver staining for proteins [15] indicated that for all three Hib porin preparations the level of protein contaminants was less than 5% (Fig. 1). When these Hib porin samples were silver stained for lipooligosaccharides (LOS) by the procedure of Tsai and Frasch [16], LOS levels were quantitated at 50–100 ng of LOS per µg of FPLC-purified porin.

2.3. Biophysical assays

Planar bilayer studies were completed using a modification of the Mueller and Rudin technique [9,17]. Two teflon chambers were separated by a teflon foil having a thickness of 100 µm and a small circular aperture of 600 µm diameter. Lipid bilayers were

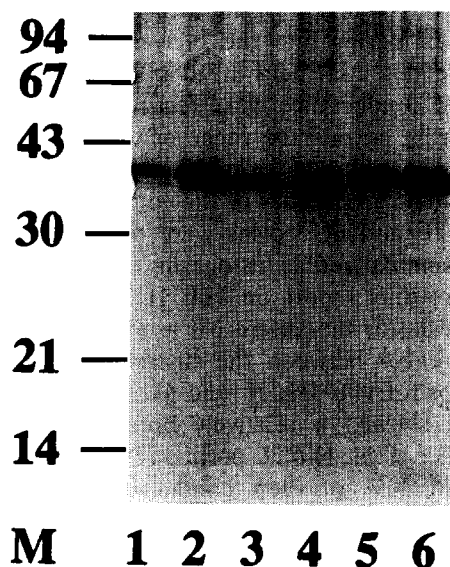


Fig. 1. SDS-PAGE of FPLC-purified porins from Hib of OMP subtypes 1H, 2L and 6U. The gel contained 13% acrylamide and was silver-stained for proteins. Lane M, molecular weight marker proteins indicated according to their molecular mass in kDa; lanes 1 and 2, 50 and 200 ng of Hib 1H porin; lanes 3 and 4, 50 and 200 ng of Hib 2L porin; lanes 5 and 6, 50 and 200 ng of Hib 6U porin, respectively.

formed across this aperture with a solution of 2.5% glyceryl monooleate (Sigma) dissolved in *n*-decane. Formation of the bilayer was monitored through a glass window on the end of one of the compartments with a light source and a microscope. Bilayer formation was indicated by the membrane's turning optically black to incident light. The porin sample was added to the aqueous phase either before membrane formation or after the membrane had turned optically black. Conductance across the membrane was measured by a fixed transmembrane potential. A pair of Ag/AgCl electrodes was inserted into solutions of 1 M KCl on both sides of the membrane. In all cases the *cis*-compartment was held at virtual ground while transmembrane potential differences were applied by the *trans*-electrode. An operational amplifier (Analog Devices, Norwood, MA; type AD 40K) was used in a current amplifier configuration such that the flow of Cl^- ions could be recorded on a strip chart recorder.

3. Results

3.1. Single channel conductance experiments

The ionic conductance properties of Hib 1H, 2L and 6U porin channels were characterized using single channel conductance experiments. To the 1 M KCl solutions bathing the planar bilayer, porin was added at a final concentration of 1 ng/ml. Shortly after the addition of porin to one or to both sides of the membrane, stepwise increases in membrane conductance were observed and were attributed to the spontaneous insertion of porins into the bilayer. With the transmembrane potential held at 10 mV, the increases in membrane conductance were recorded until the conductivity rose beyond the range of the apparatus. The membrane was then reformed and further data were recorded. The amplitudes of the conductance steps for Hib 1H, 2L and 6U porins were measured, and the data are summarized as histograms (Fig. 2). Compared to our previous report on Hib 1H porin [9], an expanded scale for the abscissa is used here to illustrate the differences between the distribution of conductance steps for Hib 1H, 2L and 6U porins. While Hib 1H porin showed a relatively broad distribution of conductance steps, Hib 2L porin and Hib 6U porin had more than 40% of their conductance steps in the 0.6–0.7 nS range.

To obtain bilayers having only a single insertion, the conductance experiments were repeated at much lower concentrations of porin. The effects of voltage on single channels were measured. At potentials of 75 mV, Hib 1H porin channels remained open for long periods of time and any fluctuation in conductance had a lifetime of less than one second (Fig. 3A). At potentials

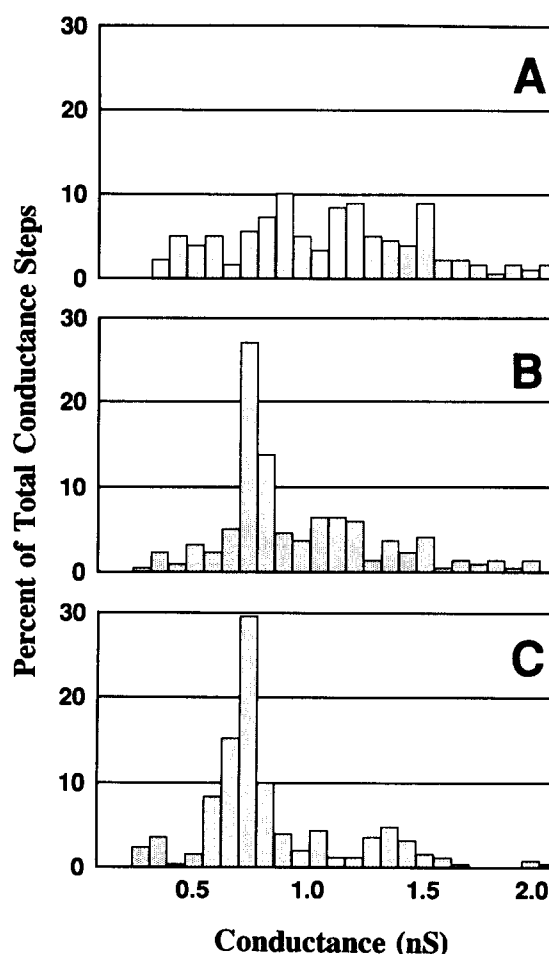


Fig. 2. Comparison of channel conductances as measured in planar bilayers for three Hib porins: 1H (panel A), 2L (panel B) and 6U (panel C). Conductance steps were recorded at a transmembrane potential of +10 mV and using 1 M KCl as the electrolyte. FPLC-purified porin at 2 $\mu\text{g}/\mu\text{l}$ in 50 mM Tris-HCl (pH 8.0), 0.1% Zwittergent Z-3,14 was diluted 500-fold into 50 mM Tris-HCl (pH 8.0). Approximately 1 μl , corresponding to 4 ng of porin, was added to the teflon chamber. The total number of conductance steps analyzed was as follows: panel A, 178; panel B, 218; panel C, 250. Conductance steps greater than 2.08 nS accounted for less than 5% of the total number of events and were not included in the analysis.

greater than 50 mV, Hib 2L porin had a high probability of shifting to one of several lower conducting channel substates (Fig. 3B). This change in conductance was fully reversible as shown by the fluctuations between different channel substates and by the return to the original conductance when the potential was shut off and then re-applied. Such a voltage effect was polarity-dependent and it occurred only at positive polarity. Voltage gating always resulted in only a partial reduction of channel conductance. In two independent experiments, unique insertions of Hib 2L porin were obtained and they showed conductances of 0.8 and 0.9 nS respectively. At high transmembrane potentials (85 and 90 mV, respectively) both of these channels shifted to substates having conductances of 0.3 nS (data not

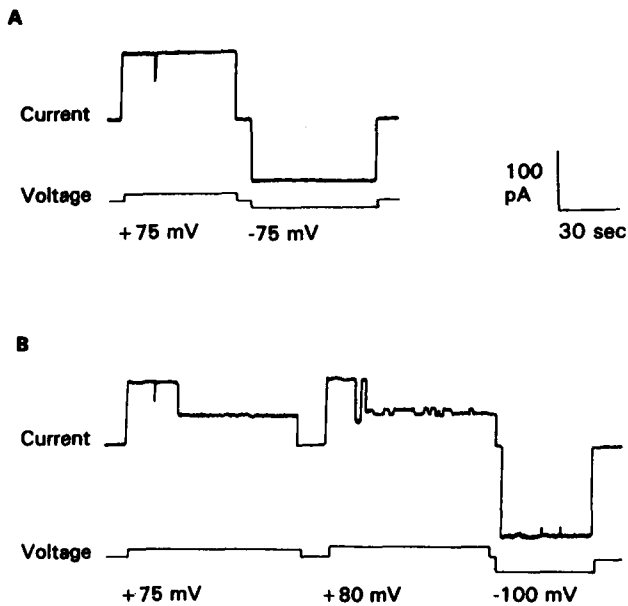


Fig. 3. Effects of voltage on single channels. FPLC-purified porin at $2 \mu\text{g}/\mu\text{l}$ in 50 mM Tris-HCl (pH 8.0), 0.1% Zwittergent Z-3,14, was diluted 5000-fold into 50 mM Tris-HCl (pH 8.0). Approximately $1 \mu\text{l}$, corresponding to 0.4 ng of porin, was added to the teflon chamber. A single insertion of either Hib 1H porin (panel A) or Hib 2L porin (panel B) into the bilayer was obtained under the influence of a membrane potential of 10 mV. Voltage steps were applied as indicated in the lower tracings. The insertion events for Hib 1H porin and Hib 2L porin both showed conductances of 1.4 nS.

shown). Occasionally, insertions of Hib 2L porin having larger conductances were detected and these too showed only a partial reduction in conductance as a result of voltage gating (Fig. 3B). For the 1.4 nS channel depicted in the tracing of Fig. 3B, channel substates having conductances of 0.8, 0.7, and 0.5 nS are distinguished. Further recording on this same channel demonstrated additional channel substates with conductances ranging from 0.8 to 0.2 nS. A total of 83 current decrement events were measured for this channel: 53 of these current decrement events involved changes in conductance of 0.1–0.2 nS; the rest of these current decrement events had magnitudes in the 0.5–1.0 nS range and showed equal distribution within this range.

3.2. Macroscopic conductance

Membranes that had stabilized with respect to porin insertions and that showed steady current levels were subjected to varying transmembrane potentials. Such experiments analyzed the effect of voltage at the macroscopic level. After membrane formation, porin was added to the *cis*-side of the planar bilayer. Once the membrane had reached steady current levels with 50–100 channels inserted, the membrane potential was shut off. The potential was then immediately re-applied and the current was recorded: after 1–2 min, the

membrane potential was returned to zero and then set to a new value in the range of -80 to $+100$ mV. The instantaneous current levels and the steady-state current levels after 1–2 min were measured and the data are expressed as current–voltage curves (Fig. 4). For Hib 1H, 2L and 6U porins, the instantaneous current flowing through the membrane responded linearly to the applied voltage and the current was symmetrical with respect to the polarity of the electric field. At voltages above 50 mV, and only at positive polarity, the instantaneous current relaxed to a lower steady-state value. For Hib 1H porin this relaxation resulted, at membrane potentials of $+75$ mV, in a steady-state

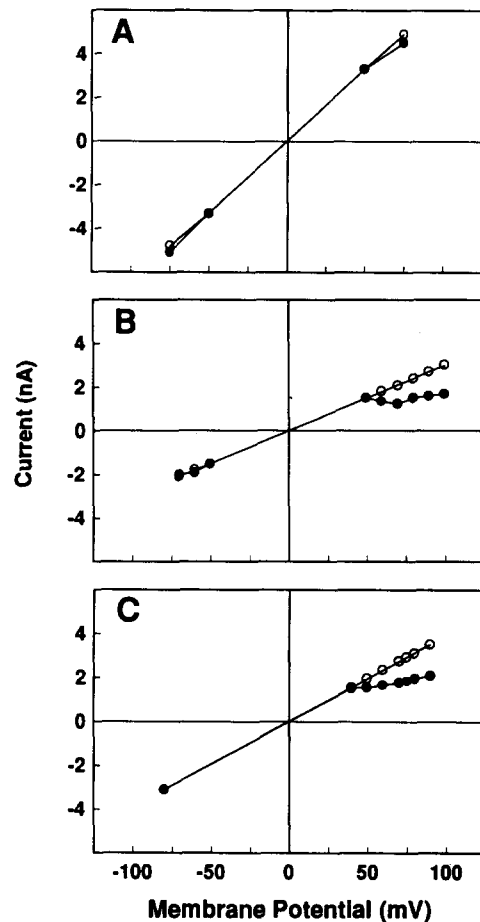


Fig. 4. Current-voltage relationships for membranes containing Hib 1H porin (panel A), Hib 2L porin (panel B), or Hib 6U porin (panel C). The line joining open circles represents the instantaneous current response; the line joining closed circles represents the steady-state current reached 1–2 minutes after application of the membrane potential. Porin concentrations were the same as for Fig. 2. To allow for porin insertion from only one side of the bilayer, the bilayers were formed prior to the addition of porin to the front teflon chamber. Since additional insertion of porin sometimes occurred between the application of voltage steps, the data were fitted to an average of the instantaneous membrane conductance. Membranes containing Hib 1H porin, Hib 2L porin or Hib 6U porin showed average instantaneous conductances of 65, 39, and 30 nS, respectively.

current that was 5–10% lower than the instantaneous current (Fig. 4A). At the same applied voltage, Hib 2L and Hib 6U porins showed a steady-state current that was 35–45% lower than the instantaneous current (Figs. 4B, C). With the membrane potential increased to +100 mV, the current across membranes containing either Hib 2L porin or Hib 6U porin did not relax to less than 50% of the instantaneous current. Polarity dependence of voltage gating for Hib 2L and 6U porins was not observed when porin was added to both sides of the membrane (data not shown).

Recordings of the relaxation of current from the instantaneous level to the steady-state level are shown in Fig. 5. Relaxation times were voltage-dependent: the

higher the voltage, the faster the relaxation time (Figs. 5B, 5C). Relaxation was also fully reversible: when the potential was shut off momentarily and then re-applied, the membrane returned to its original conductance. Current relaxation occurred in a cascade of small steps. In order better to resolve the conductance amplitude of these closing steps, we obtained bilayers incorporating fewer than 20 porins. These bilayers were subjected to voltage steps of 50–85 mV and the conductance amplitudes of the ensuing channel-closing steps were calculated. The data are presented as histograms (Fig. 6). For both Hib 2L and 6U porins, most of these conductance steps were in the 0.8–1.2 nS range.

4. Discussion

Although the physiological significance of voltage gating of bacterial porins remains controversial [4], this report and many others [18–23] document the sensitivity to voltage by these proteins which are isolated from the bacterial outer membrane. There is at present little understanding of changes in protein structure that can be induced by different applied voltages or of changes in amino-acid sequences that may affect voltage gating. The objective of this paper was to determine the voltage sensitivities of three naturally occurring sequence variants of porins from Hib. Based on published DNA sequence data [24] and our confirmation of these sequences, the *ompP2* gene for Hib 2L porin differs from its 1H counterpart by a single base pair, resulting in the amino-acid change Arg¹⁶⁶Gln. The *ompP2* gene for Hib 6U porin encodes a protein that differs from the two other porins by 10 amino acids, including the alteration Arg¹⁶⁶Leu.

Following extraction of bacterial cells with CTB and FPLC-based purification of the three sequence variants of Hib porins, an evaluation of the conformation of the porins was necessary. Our previous studies [8] measured the molecular weight exclusion limit that was attributed either to isolated outer membranes that had not been subjected to CTB, or to extracted and purified porins. The experimental values for both were identical, 1400 Da, and so it was proposed that the conditions for extraction with CTB did not adversely affect the proteins' pore-forming functions. We also assessed the secondary structure of Hib porins by spectroscopic techniques including circular dichroism and Fourier transform infrared spectroscopy. Because there were no discernable differences in the spectroscopic properties of Hib porins (our unpublished data) compared to the spectroscopic properties of other well characterized porins [25,26], we propose that the native secondary structure, primarily β -sheet, was not perturbed by our purification protocols. The porins were

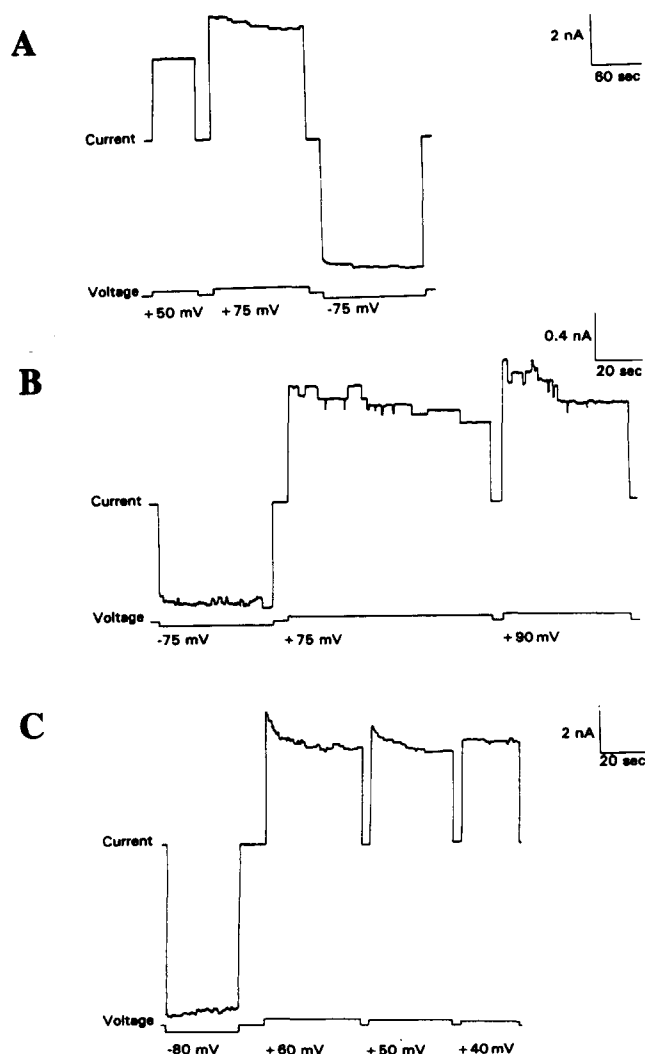


Fig. 5. Current relaxation of membranes containing Hib porin. Voltage steps were applied as indicated in the lower tracings and the current monitored such that individual conductance steps were resolved during current relaxation to steady-state. Porin was added to the teflon chamber as explained in Fig. 4. Bilayers incorporating Hib 1H porin (panel A), Hib 2L porin (panel B) or Hib 6U porin (panel C) showed instantaneous conductances of 65, 13 and 50 nS, respectively.

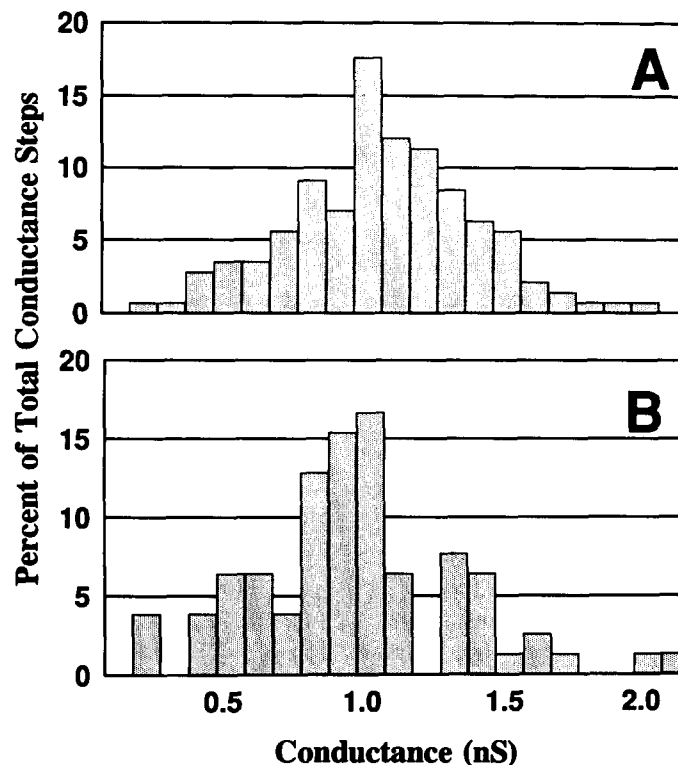


Fig. 6. Size distributions of conductance steps occurring during current relaxation for membranes incorporating Hib 2L porin (panel A), and Hib 6U porin (panel B). The channel-closing events were recorded after membranes, with 2–20 porins inserted, had their transmembrane potential shifted from 0 to 50–85 mV. The total number of channel closing events was 142 and 83 for Hib 2L porin and Hib 6U porin, respectively. Conditions for addition of porin to the teflon chamber were the same as for Fig. 2.

therefore suitable for our further biophysical studies.

While *E. coli* porins form trimers that remain stable at temperatures up to 70°C [25], Hib porin was shown to migrate as a monomer upon SDS-polyacrylamide gel electrophoresis even when solubilized at room temperature [27]. Using the cross-linking reagent dithio-bis(succinimidyl propionate) only a small proportion of the Hib porin molecules were found as cross-linked trimers [27]. Clairoux et al. [28] reported that by using sarkosyl and lauryl sulfobetaine for extraction and purification, porins from various *Haemophilus influenzae* isolates (nontypeable strains as well as type b and type c strains) had greater than 40% of their conductance steps in the 2.0–2.5 nS range. Lower conductance values were seen when porin was treated with a harsh detergent such as SDS: 50% of conductance steps were in the 0.75–1.25 nS range. They proposed that Hib porin formed unstable trimers and that by treatment with SDS the trimers dissociated into functional monomers. Most of the conductance steps that we observed for Hib 1H, 2L and 6U porins were in the 0.7–1.1 nS range. Our results suggest that for all three sequence variants of porins, trimers were dissociated by CTB during extraction and purification and that we have primarily observed the insertion of monomers into the synthetic bilayer. That porin can function as a

monomer is not unexpected as porin crystal structures show that each monomer forms its own pore [6,7].

Compared to Hib 1H porin, the Hib 2L and 6U porins showed a much narrower distribution of conductance steps (Fig. 2). The electrical properties of Hib porin may be influenced by the electric field produced by the numerous negatively charged groups on LOS [29]. The wide distribution of conductance steps seen for Hib 1H porin might then be attributed to variation in the number of LOS molecules associated with 1H porin. The Hib 2L and 6U porins may differ from Hib 1H porin in their affinity for LOS.

While voltage gating of single channels resulted in a partial closing of the channels, those within a multimer closed cooperatively as determined by single channel measurements and by macroscopic conductance measurements. Fig. 3B shows an example of a single insertion of Hib 2L porin with a relatively large conductance of 1.4 nS, suggesting that a multimer of channels had inserted. During voltage gating this multimer did not show several equivalent current decrement events as would have been expected if the monomers were independently voltage-gated. Furthermore, during current relaxation at the macroscopic level, Hib 2L and 6U porins showed conductance steps in the 0.8–1.2 nS range. Such a conductance step is larger than the

conductance of a single channel (0.7–0.8 nS), yet current relaxation at the macroscopic level rarely resulted in more than 50% reduction in conductance. Although it cannot be excluded that channels within oligomers could close more often than those of monomers, these results suggest that Hib porin monomers could oligomerize once in the lipid environment and that the 0.8–1.2 nS conductance steps observed during current relaxation could be due to cooperative interactions among porin monomers. Such interactions would result in the simultaneous partial closing of porin channels assembled into multimers.

Our results represent the first description of Hib porin voltage gating. The gating is characterised by cooperative interactions, by polarity dependence, and by the presence of multiple long-lived substates. Numerous reports describe the voltage gating of porins from *E. coli* [19,20,23] and *N. gonorrhoeae* [21]. In contrast to Hib porins, these *E. coli* and *N. gonorrhoeae* channels exist in two stable conformations, open and closed. Substates were observed to have lifetimes that are in the range of milliseconds. Furthermore, with each of these *E. coli* and *N. gonorrhoeae* porins, the closed state has a conductance value that is just a few percent of the open-state conductance. While channels within a trimer can close independently of each other [21,23], there have been reports of cooperative interactions among channel monomers as well as among porin trimers [19,23]. Conflicting reports have appeared with regards to the polarity dependence of voltage gating for the *E. coli* and *N. gonorrhoeae* porins. In general, studies relying on the technique of patch-clamping of giant proteoliposomes show a polarity dependence [18,19]. Those studies that involved reconstitution into planar bilayers showed polarity-independent gating [20,21,23]. These conflicting reports may be resolved by proposing different mechanisms whereby a given porin is affected by voltage. The mechanism observed could be dependent upon experimental conditions such as the strength of the membrane potential used to induce voltage gating or the methods of reconstitution.

The polarity-dependent voltage gating that was observed at the macroscopic level suggested that Hib 2L porin and Hib 6U porin inserted into the bilayer in an oriented rather than in a random manner. Morgan et al. [22] observed a similar phenomenon with a crude *E. coli* porin preparation containing both OmpF and OmpC. They hypothesized that oriented insertion occurred because porin was complexed with LPS and inserted into planar bilayers such that the hydrophilic polysaccharide moiety of LPS remained in the aqueous medium bathing the membrane. However, asymmetric insertion into preformed lipid vesicles has been reported for *E. coli* OmpA purified free of LPS [30]. In the latter case, the authors concluded that oriented

insertion occurred for reasons inherent to the mechanism by which OmpA inserts into membranes. Such a mechanism might be common to all outer membrane proteins that are organized as transmembrane β -barrels.

Our model for the secondary structure of Hib porin was based in part on results from epitope scanning of synthetic hexapeptides with seven MABs [11]. The epitope scanning studies showed that amino acids 162–171 and 165–172 of Hib porin comprise the epitopes recognized by MABs POR.4 and POR.5, respectively. We assigned Arg¹⁶⁶ to the fourth surface-exposed loop and demonstrated that Arg¹⁶⁶ is critical to recognition by MAB POR.4. By flow cytometry, MAB POR.4 was shown to bind to intact Hib cells that displayed the 1H porin, thereby confirming the surface-exposure of Arg¹⁶⁶. Furthermore, while the binding of MAB POR.4 to intact Hib cells that displayed either 2L porin or 6U porin was not detectable by flow cytometry, MAB POR.5 showed similar affinity for Hib cells displaying either 1H or 2L porin. Thus the Arg¹⁶⁶Gln change did not result in any large-scale structural changes. Hib 1H porin differs from Hib 2L porin by one surface-exposed residue and yet these two porins show pronounced differences in voltage gating. That such a minor change in the primary structure of Hib porin can affect voltage sensitivity suggests that the conformational changes that occur during voltage gating do not necessarily involve gross alterations of pore structure but rather might involve changes of localized regions of porin.

How might Arg¹⁶⁶ influence voltage gating of the porin channel? One possibility is that the positively charged Arg¹⁶⁶ residue forms an ionic bond that serves to restrict the motion of one or more of the surface-exposed loops. The absence of this ionic bond in Hib 2L porin would allow one or more of the surface-exposed loops to move towards the lumen of the pore in the presence of an electric field.

Discrete changes in porin channel size have been reported as responses to a variety of stimuli: membrane potential [18–21,23], osmotic pressure [31,32] and pH [33]. An understanding of the structural basis for this conformational plasticity is desirable. Our evidence now implicates at least one surface-exposed loop of Hib porin as being involved in voltage-dependent conformational changes. Determination of the high resolution structure of Hib porin will allow for an assessment of the molecular context of the Arg¹⁶⁶ residue and will test our interpretations of the structural dynamics of Hib porin.

Acknowledgements

This research was supported by grant MT-6911 to J.W.C. from the Medical Research Council, Canada.

Facilities at the Groupe de Recherche en Transport Membranaire, Université de Montréal, are supported by NSERC research grant GP9598 to R.L. We appreciate the critical review of Dr. R.C. Stewart.

References

- [1] Nikaido, H. and Vaara, M. (1985) *Microbiol. Rev.* 49, 1–32.
- [2] Jeanteur, D., Lakey, J.H. and Pattus, F. (1991) *Mol. Microbiol.* 5, 2153–2164.
- [3] Benz, R. (1985) *CRC Crit. Rev. Biochem.* 19, 145–190.
- [4] Jap, B.K. and Walian, P.J. (1990) *Q. Rev. Biophys.* 23, 367–403.
- [5] Nikaido, H. (1992) *Mol. Microbiol.* 6, 435–442.
- [6] Cowan, S.W., Schirmer, T., Rummel, G., Steiert, M., Ghosh, R., Pauptit, R.A., Jansonius, J.N. and Rosenbusch, J.P. (1992) *Nature* 358, 727–733.
- [7] Weiss, M.S., Abele, U., Weckesser, J., Welte, W., Schiltz, E. and Schulz, G.E. (1991) *Science* 254, 1627–1630.
- [8] Vachon, V., Lyew, D.J. and Coulton, J.W. (1985) *J. Bacteriol.* 162, 918–924.
- [9] Vachon, V., Laprade, R. and Coulton, J.W. (1986) *Biochim. Biophys. Acta* 861, 74–82.
- [10] Srikumar, R., Chin, A.C., Vachon, V., Richardson, C.D., Ratcliffe, M.J.H., Saarinen, L., Käyhty, H., Mäkelä, P.H. and Coulton, J.W. (1992) *Mol. Microbiol.* 6, 665–676.
- [11] Srikumar, R., Dahan, D., Gras, M.F., Ratcliffe, M.J.H., Van Alphen, L. and Coulton, J.W. (1992) *J. Bacteriol.* 174, 4007–4016.
- [12] van Alphen, L., Eijk, P., Geelan-van den Broek, L. and Dankert, J. (1991) *Infect. Immunol.* 59, 247–252.
- [13] Smith, P.K., Krohn, R.I., Hermanson, G.T., Mallia, A.K., Gartner, F.H., Provenzano, M.D., Fujimoto, E.K., Goeke, N.M., Olsen, B.J. and Klenk, D.C. (1985) *Anal. Biochem.* 150, 76–85.
- [14] Lugtenberg, B., Meijers, J., Peters, R. and Van der Hoek, P. (1975) *FEBS Lett.* 58, 254–258.
- [15] Morrissey, J.H. (1981) *Anal. Biochem.* 117, 307–310.
- [16] Tsai, C.-M. and Frasch, C.E. (1982) *Anal. Biochem.* 119, 115–119.
- [17] Mueller, P., Rudin, D.O., Tien, H.T. and Westcott, W.C. (1963) *J. Phys. Chem.* 67, 534–535.
- [18] Delcour, A.H., Adler, J. and Kung, C. (1991) *J. Membr. Biol.* 119, 267–275.
- [19] Delcour, A.H., Adler, J., Kung, C. and Martinac, B. (1992) *FEBS Lett.* 304, 216–220.
- [20] Lakey, J.H. and Pattus, F. (1989) *Eur. J. Biochem.* 186, 303–308.
- [21] Mauro, A., Blake, M. and Labarca, P. (1988) *Proc. Natl. Acad. Sci. USA* 85, 1071–1075.
- [22] Morgan, H., Lonsdale, J.T. and Alder, G. (1990) *Biochim. Biophys. Acta* 1021, 175–181.
- [23] Schindler, H. and Rosenbusch, J.P. (1981) *Proc. Natl. Acad. Sci. USA* 78, 2302–2306.
- [24] Munson, R., Jr., Bailey, C. and Gras, S. (1989) *Mol. Microbiol.* 3, 1797–1803.
- [25] Eisele, J.-L. and Rosenbusch, J.P. (1990) *J. Biol. Chem.* 265, 10217–10220.
- [26] Navedryk, E., Garavito, R.M. and Breton, J. (1988) *Biophys. J.* 53, 671–676.
- [27] Vachon, V., Kristjanson, D.N. and Coulton, J.W. (1988) *Can. J. Microbiol.* 34, 134–140.
- [28] Clairoux, N., Picard, M., Brochu, A., Rousseau, N., Gourde, P., Beauchamp, D., Parr, T.R., Jr., Bergeron, M.G. and Malouin, F. (1992) *Antimicrobiol. Agents Chemother.* 36, 1504–1513.
- [29] Jap, B.K. (1989) *J. Mol. Biol.* 205, 407–419.
- [30] Surrey, T. and Jähnig, F. (1992) *Proc. Natl. Acad. Sci. USA* 89, 7457–7461.
- [31] Buechner, M., Delcour, A.H., Martinac, B. and Adler, J. (1990) *Biochim. Biophys. Acta* 1024, 111–121.
- [32] Martinac, B., Buechner, M., Delcour, A.H., Adler, J. and Kung, C. (1987) *Proc. Natl. Acad. Sci. USA* 84, 2297–2301.
- [33] Todt, J.C., Rocque, W.J. and McGroarty, E.J. (1992) *Biochemistry* 31, 10471–10478.